Complexity Project: The Oslo Model

Sulaiman Rasool, CID : 01519545

20th February, 2021

Abstract: This report studies the behaviour of the Oslo model algorithm to understand the avalanche-size probability, the general framework of scaling and the consistency of the result with systems displaying self-organised criticality. This report shows that the average height of system scales proportional to the system size in the steady state and details that the height of the system is proportional to the square root of time during the transient state. The report then discusses the scaling behaviour of height in the transient state and determines the scaling constants $a_0 = 1.727$ and $w_1 = 0.654$. The report then discusses about the avalanche-size probability showing that this can be approximated by a power-law decay and determines the values for the avalanche dimension, D = 2.141 $\pm$ 0.025 and the avalanche-size exponent, $\tau_s = 1.542$. The report shows that the scaling is consistent with a boundary driven system and that the Oslo model self-organises in a steady state displaying self-organised criticality.

Word count: 2440 words in report (excluding front page, figure captions, table captions, acknowledgement and bibliography).

1 Introduction

The Oslo model is one of the simplest models that display self-organised criticality, the behaviour of slowly driven systems to organise themselves into susceptible states. This aim of this report is to study the behaviour of the Oslo model algorithm I implemented and to understand the avalanche-size probability, the general framework of scaling and data collapse and the consistency of the results with systems displaying self-organised criticality.

1.1 Outline

The report contains the following sections: The introduction to the project. Implementation of the Oslo model, describing tests performed on the program. The height of the pile, section detailing the analysis performed on the height of the pile. The avalanche-size probability, detailing the measurements of the avalanche-size probability and associated moments including the relevant theory and results. The final section is a conclusion.

2 Implementation of the Oslo model

This section details the tests performed on the Oslo model algorithm as part of Task (1).

2.1 Test: 1

Measuring the average height of the system at site i = 1 in the steady state. For p $=\frac{1}{2}$, the expected height for the system size L = 16 is 26.5 and for L = 32 is 53.9.

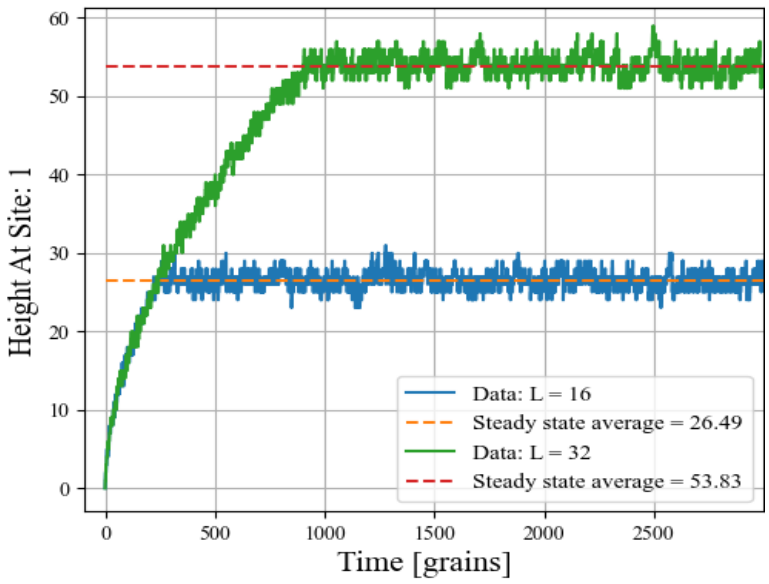

Figure 1: Height plot, showing the height of the system at site i = 1 as a function of time, measured in the number of grains added to the system. The plot shows the transient(rising curve) and steady state of the height for the system size L = 16 and L = 32. The plot also shows the average steady state values for each system.

Figure 1 shows that for L = 16 the steady state average is 26.55 and for L = 32 the average is 53.9. This corroborates with the expected values.

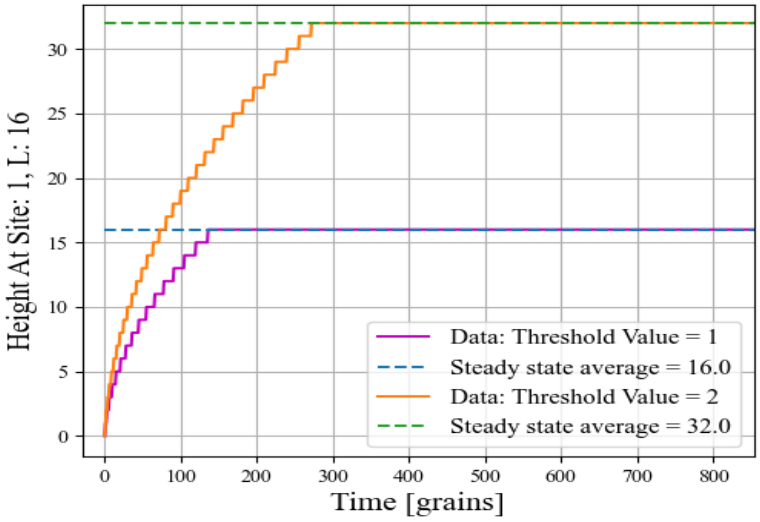

Figure 2: Height plot, showing the height of the system at site i = 1 as a function of time, measured in the number of grains added to the system. The plot shows the transient and steady state of the height for the system size L = 16 with a threshold probability of p = 1 and p = 0. The plot also shows the average steady state values for each system.

2.2 Test: 2

Test 2 repeats Test 1 for different p values. For p = 1, the threshold slope values can only be 1 thus $h_1 = L$. For p = 0, the threshold slope values can only be 2 and hence $h_1 = 2L$. For L = 16 the calculated values for p = 0 is $h_1 = 16$ and for p = 1 is $h_1 = 32$.

The results in figure (2) show that for p = 1 is h_1 =16 and for p = 0 the $h_1 = 32$. This corroborates with the calculated values.

2.3 Test: 3

Test 3 measures the average avalanche size as a function of the system size L to verify the theory that shows that the average avalanche size, $\langle s \rangle$, is proportional to the system size.

The gradient of the linear fit in figure (3), m = 1.0 ± 0.003, implies that the relation between $\langle s \rangle$ and L is linear. This corroborates with the theoretical background.

3 The height of the pile

This section measures the height of the pile and performs measurements to analyse the Oslo model.

3.1 Task 2a

Task 2a measures the height of the pile, h(t; L) given by, In the algorithm, the height at site i = 1. was measured directly by recording the changes to the site.

3.1.1 Results

Figure (4) shows the transient state which is the evolution of the height until the first grain has left the system and the steady state . The transient state will keep increasing in height until the first grain has left hence each configuration of heights is unique. The

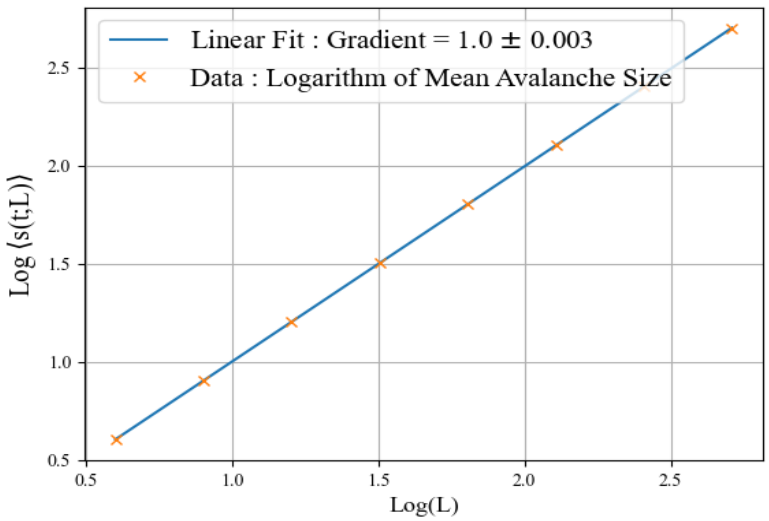

Figure 3: Average avalanche plot, showing the logarithm of the average avalanche size as a function of the logarithm of the system size. The gradient of the linear fit implies that $\langle s \rangle$ scales linearly with respect to L.

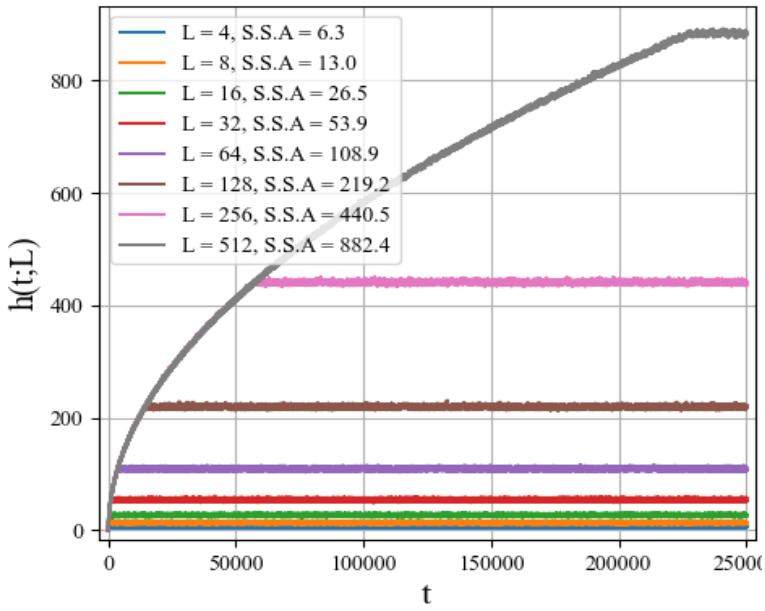

Figure 4: Height plot, showing the height of the system at site i = 1, h(t; L), as a function of time for different system sizes. The plot shows the evolution of the transient and steady state of h(t; L) and details the steady state average (S.S.A) of each system. The figure implies that the transient evolution is identical for each system until a steady state has been reached.

transient configuration of each system evolve the same and independent of the system size the steady state. The recurrent configuration of heights in steady is determined by the system size. This is seen in figure 3 as the steady state average (S.S.A) of each system increases as L increases.

3.2 Task 2b

Task 2b investigates how the average cross-over time, $\langle t_c(L)\rangle$, scales with L for L >> 1. The cross-over time, t_c, is defined as the number of grains in the system before an added grain induces a grain to leave the system.

3.2.1 Results

Average cross-over time, figure 5 (a), shows that $\langle t_c(L)\rangle$ increases at a greater rate for larger L and by plotting a quadratic fit, $o(n^2)$, we see that the data is of $o(n^2)$.

To corroborate the result, I plotted Log($\langle t_c(L)\rangle$) as a function of Log(L) shown in figure 5 (b). The figure shows a linear fit that has a gradient, m = 1.99 $\pm$ 0.018. The results imply that $\langle t_c(L)\rangle \propto L^2$ as the gradient is approximately 2 for $L >> 1$ and corroborates the findings above.

3.3 Task 2c

Task 2c devises a theoretical argument to show scaling of the height and the cross-over time.

3.3.1 Height scaling

Confine the threshold value to only 1 and select L = 4, resulting in $\langle h(t;L)\rangle = 4$. For L = 16 we expect $\langle h(t;L)\rangle = 16$. For a threshold value of only 2 when L = 4 $\langle h(t;L)\rangle = 8$ and for L = 16 $\langle h(t;L)\rangle = 32$. Figure 2 shows that $\langle h(t;L)\rangle$ scales linearly with system size. In the Oslo model, the threshold value can take 1 or 2 with an equal probability therefore if $\langle h(t;L)\rangle$ scales linearly with a threshold value of 1 and 2 then any value in between them must also scale linearly so,

$$\langle h(t;L)\rangle = \langle z\rangle L \tag{1}$$

for $L >> 1$, where $\langle z\rangle$ is the average slope of the system in the steady state.

3.3.2 Cross-over time scaling

The system is approximated as a right angle triangle with base L and height h(t; L). The area of the triangle, $\langle t_c(L)\rangle$is given by,

$$\langle t_c(L)\rangle = \frac{1}{2}h(t;L)L \tag{2}$$

we substitute for h(t; L) to obtain,

$$\langle t_c(L)\rangle = \frac{1}{2}\langle z\rangle L^2 \tag{3}$$

this shows that $\langle t_c(L)\rangle \propto L^2$ as $\frac{1}{2}\langle z\rangle$ is a constant. The results here are further corroborated by the findings in figure 5 (b).

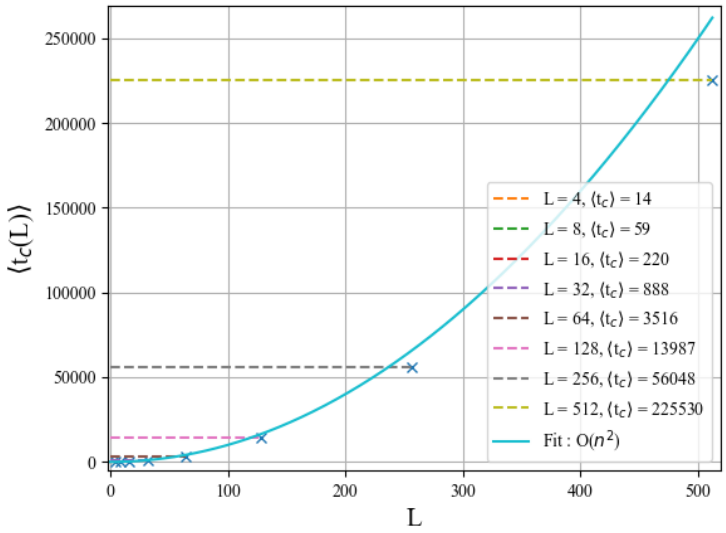

(a) Average cross-over time

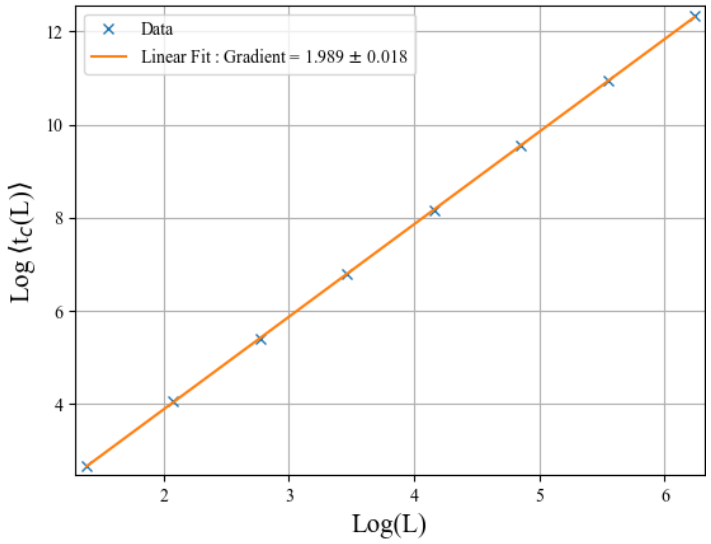

(b) Logarithm of cross-over time

Figure 5: Cross-over time analysis for L = 4, 8,16, 32, 64, 128, 256, 512. Figure (a) shows the average cross-over time, $\langle t_c \rangle(L)$, as a function of L. The plot shows $\langle t_c(L) \rangle$ for each L. The plot also shows a quadratic fit, $o(n^2)$ to the data. The figure implies that for L = 4 to L = 128 the $\langle t_c(L) \rangle$ is approximately quadratic and shows that there is a small deviation for L larger than 128. Figure(b) shows the logarithm of average cross-over time as a function of the logarithm of the system size. The plot shows a linear fit to the data with a gradient, m = 1.99 ± 0.018. The figure implies that $\langle t_c(L) \rangle$ scales proportional to L^2 as m can be approximated to 2.

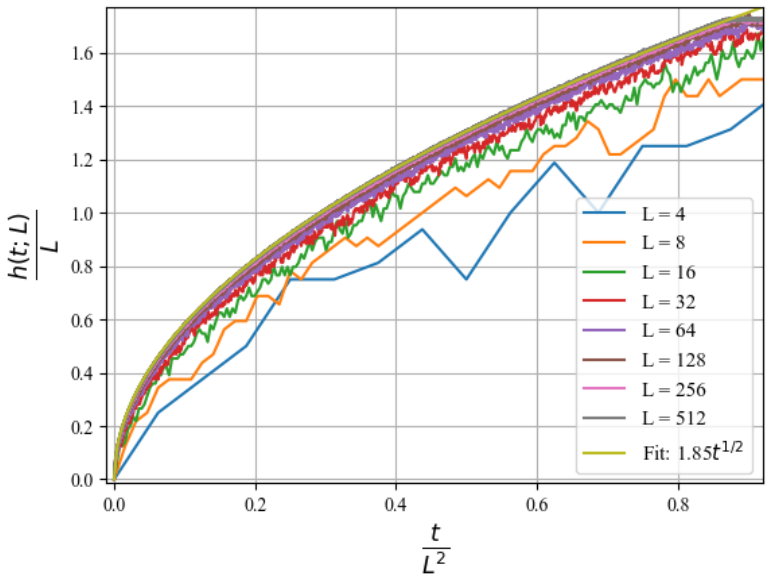

Figure 6: Data collapse plot, showing the processed height divide by the system size, $\frac{\tilde{h}(t;L)}{L}$ as a function of time divided by system size squared, $\frac{t}{L^2}$. The plots shows a scaled fit, $1.85t^{\frac{1}{2}}$. The figure implies for the transient state the processed height scales as $\tilde{h} \propto t^{\frac{1}{2}}$ and for the steady state $\frac{\tilde{h}(t;L)}{L}$ is approximately constant with a value of 1.73.

3.4 Task 2d

Task 2d produces a data collapse for the processed height (average height of different realisations) using a scaling function $\mathcal{F}$ such that,

$$\tilde{h}(t;L) = something\mathcal{F}(argument) \tag{4}$$

where something and argument needs to be determined.

3.4.1 Results

Task 2c showed that $\langle h \rangle \propto$ L therefore the y-axis is collapsed by dividing $\tilde{h}(t;L)$ by L. Task 2c also showed that $\langle t_c(L) \rangle \propto L^2$ and as $\langle t_c(L) \rangle$ is the the only characteristic timescale, t is divided by L^2 to collapse the x-axis. Collating the expressions, equation (4) can be expressed as,

$$\tilde{h}(t;L) = L\mathcal{F}\left(\frac{t}{L^2}\right) \tag{5}$$

where L is something and the argument is $\frac{t}{L^2}$.

Figure 6, implies that as L increases the systems converge to an experimental fit, $\tilde{h} = 1.85\sqrt{t}$ for the transient state of the system. The fit was derived from the behaviour of the scaling function $\mathcal{F}(x)$ where x is $\frac{t}{L^2}$. For x >>1 the system for any L is in the steady state hence $\mathcal{F}(x)$ is constant so that $\tilde{h} \propto L$ as seen from Task 2c. This result is seen in figure 6 as all curves approximately converge to 1.73. For small arguments, x << 1 the systems are in the transient state and as such $\mathcal{F}(x)$ must behave so that $\tilde{h}$ in the transient state evolves independent of L which is a result we have seen in Task 2a. We assert that $\mathcal{F}(x) \propto \frac{\sqrt{t}}{L}$ and simplifies equation (5) to,

$$\tilde{h}(t;L) = A\sqrt{t} \tag{6}$$

where A is a constant determined by coordinates at the cross-over time. A = 1.85, as shown in figure 7 hence the results imply that $\tilde{h} \propto \sqrt{t}$.

3.5 Task 2e

Task 2e investigates the signs of corrections to scaling for the average height given by,

$$\langle h(t;L)\rangle = a_0 L(1 - a_1 L^{-w_1}) \tag{7}$$

where a_0, a_1 and w_1 are constants to be determined. Two procedures were used to address Task 2e.

3.5.1 Curve Fit Method

This method uses scipy.optimise.curve.fit a scipy package which uses non-linear least squares to fit a function f to the data. The method used the following function,

$$\frac{\langle h(t;L)\rangle}{L} = a_0(1 - a_1 L^{-w_1}) \tag{8}$$

where the RHS is the function f to be optimised.

3.5.2 Derived Method

Equation (1) shows that for large L equation (7) reduces to,

$$\langle h(t;L)\rangle = a_0 L \tag{9}$$

as $w_1 >> 0$ and has less contribution to large values of L. Then $h\langle(t;L)\rangle$ is plotted as a function of L and the gradient represents a_0. To obtain w_1 and a_1, equation (7) is manipulated so,

$$Log(L - \frac{\langle h(t;L)\rangle}{a_0}) = (1 - w_1)Log(L) + Log(a_1) \tag{10}$$

here a_0 is now known. The LHS of the equation is plotted against Log(L). A straight line is fitted for relatively small values of L for L = 4, 8, 16, 32 and 64. The gradient of the line = $1 - w_1$ and the y-intercept = Log(a_1).

3.5.3 Results

Figure 7 (a), shows that $a_0 = 1.727 \pm 0.234$ which is the gradient of the linear fit.

Figure 7 (b) shows a linear fit for L = 4, 8, 16, 32 and 64. Utilising the gradient, w_1 = 0.653 ± 0.085 and from the Y intercept $a_1 = 0.225$. Table (1) collates the values of the constants.

Figure 8 shows three different data sets; Data refers to the actual data, Curve fit plotted using the Curve Fit method and Derived method fit plotted using the Derived method. The figure implies that there is scaling corrections of the form in equation (8) and of higher orders. The figure also implies that the Derived method produced more accurate constants as it more closely follows the trajectory described by the actual data.

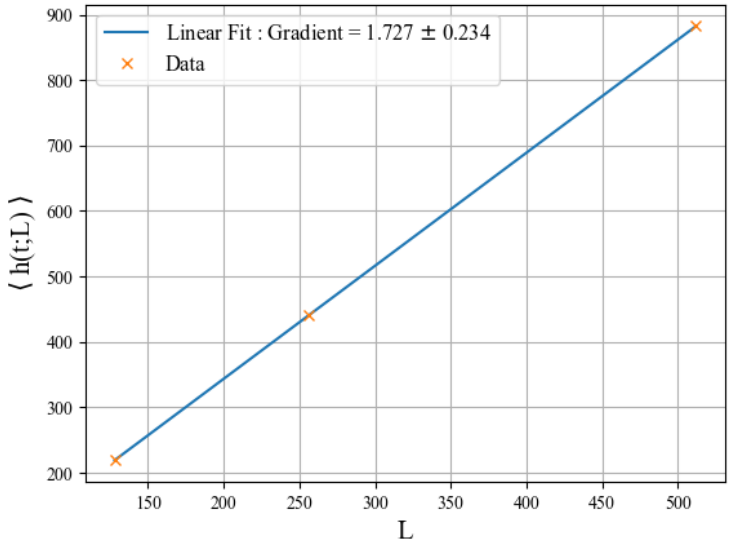

(a) Average height plot

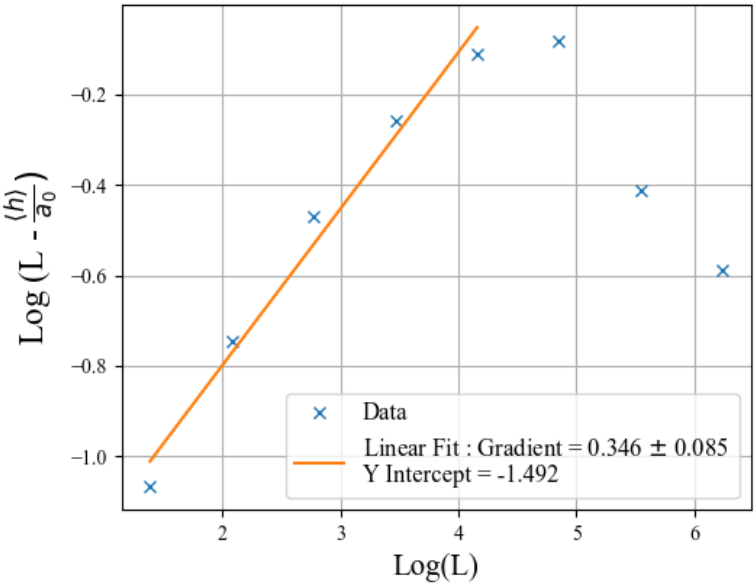

(b)

Figure 7: Figure (a) shows the average height,$\langle h(t;L)\rangle$, as a function of L for values of L = 128, 256 and 512. The plot shows a linear fit with a gradient, m = 1.727 ± 0.234. The figure is used to calculate the scaling a_0 derived from m. The derived value of $a_0 = 1.727 \pm 0.234$. Figure (b) shows the Logarithm of $(L - \frac{\langle h(t;L)\rangle}{a_0})$ as a function of Logarithm of L. The plot shows a linear fit for values of L = 4, 8, 16, 32 and 64 with a gradient, m = 0.346 ± 0.085 with a Y intercept, c = -1.492. The figure is used to calculate the scaling constant w_1 and a_1 derived in equation (10). The values derived from the figure are $w_1 = 0.653 \pm 0.085$ and $a_1 = 0.225$.

Estimations of Scaling Constants			
Method	a_0	w_1	a_1
Curve Fit Method	1.74	0.511	0.332
Derived Method	1.727	0.654	0.225

Table 1: Estimations of Scaling Constants table, showing the values estimated for the scaling constants discussed in equation (10) using two methods, Curve Fit method described in section 3.5.1 and the Derived Method described in section 3.5.2

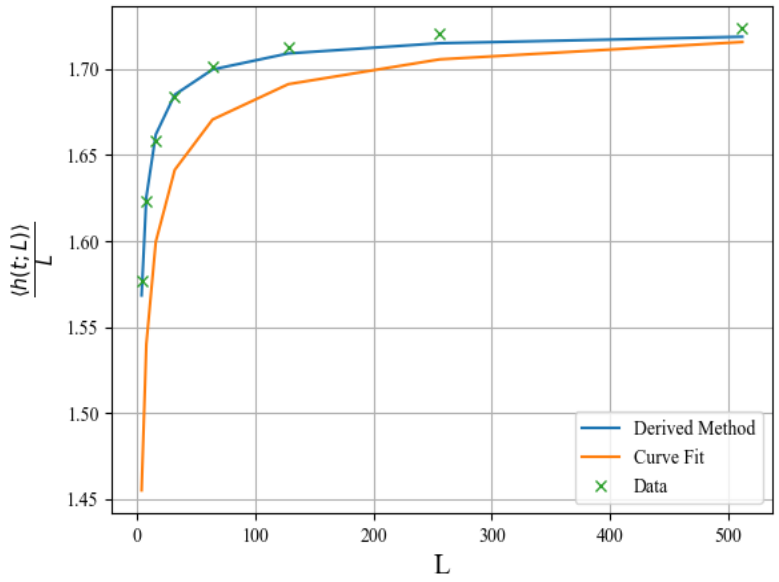

Figure 8: Average height plot, showing the average height divide by system size as a function of system size. The plot shows three different data points; Data represents the actual simulated data for which we investigate scaling, Curve Fit is data that was plotted using the scaling constants determined from the Curve Fit method and Derived fit is data that was plotted using the scaling constants determined from the Derived method. The figure implies that there are corrections to scaling as the data deviates from the two methods.

3.6 Task 2f

Task 2f investigates scaling of the standard deviation of the height, $\sigma_h(L)$ with the L, calculated using,

$$\sigma_h(h) = \sqrt{\langle h^2(t;L)\rangle_t - \langle h(t;L)\rangle_t^2} \tag{11}$$

where $\langle h^2(t;L)\rangle_t$ is the average of the square of the heights.

3.6.1 Results

Figure 9 shows a linear fit with gradient, m = 0.259 ± 0.041 and implies that $\sigma_h \propto L^{0.259}$. Using the observations made in Task 2e and 2f , when L $\to \infty$ the average slope approaches a_0 and as L $\to \infty$ σ_h tends to infinity.

3.7 Task 2g

Task 2g investigates the height probability, P(h; L) given by,

$$P(h;L) = \frac{No.\ of\ observed\ configurations\ with\ height\ h\ in\ pile\ size\ L}{Total\ no.\ observed\ configurations} \tag{12}$$

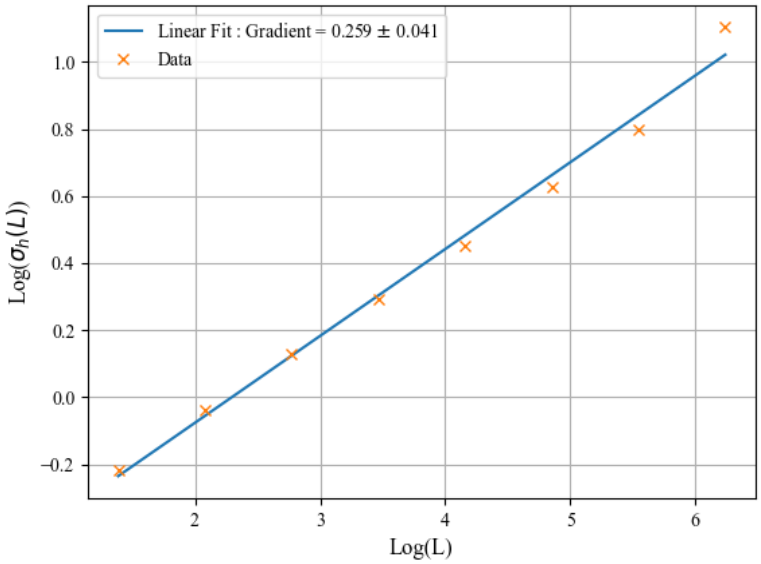

Figure 9: Standard deviation plot, showing the logarithm of the standard deviation as a function of the logarithm of system size. The plot shows a linear fit with gradient, m = 0.259 ± 0.041. The figure implies that the $\sigma_h \propto L^{0.259}$.

3.7.1 Task 2g(a) results

In this section of the task, z_i is assumed to be an independent and identically distributed random variable with finite variance. As a result P(h; L) is expected to be distributed as a Gaussian due to the central limit theorem which states that the normalised sum of independent variables tends towards a normal distribution. The scaling of σ_h can be calculated using the error propagation formula given by,

$$\sigma_h(L)^2 = \sum_{i=1}^{L} \left(\frac{\partial h}{\partial z_i} \right)^2 \sigma_{z_i}^2 \tag{13}$$

where σ_{z_i} is the error in the slope at site i. Due to the theoretical assumptions that z_i are identically distributed the differential is = 1 and the sum of i = 1 to L becomes L hence,

$$\sigma_h(L) = \sigma_{z_i} \sqrt{L} \tag{14}$$

which shows that $\sigma_h(L) \propto \sqrt{L}$.

3.7.2 Task 2g(b) results

Figure 10 (a), implies that as L increases the maximum P(h; L) decreases due to larger systems having access to a larger range of heights and that the total probability must sum to 1. To produce a data collapse we use the theoretical prediction the systems must tend to a Gaussian of the form,

$$P(h; L) = \frac{1}{\sigma_h \sqrt{2\pi}} e^{-\frac{1}{2}k^2} \tag{15}$$

where k = $\frac{h - \langle h \rangle}{\sigma_h}$. The data can be collapsed by plotting $\sigma_h P(h; L)$ as a function of k which ensures that all the systems are centred about 0 and scaled.

Data collapse, 10 (b), shows a Gaussian fit with $\mu = 0$ and $\sigma = 1$. The figure implies the data does not corroborate with the theoretical prediction as all system sizes deviate

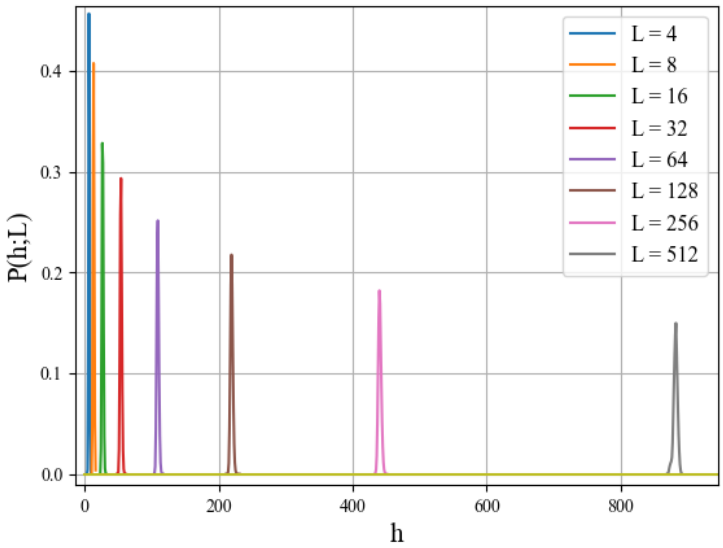

(a) Height probability plot

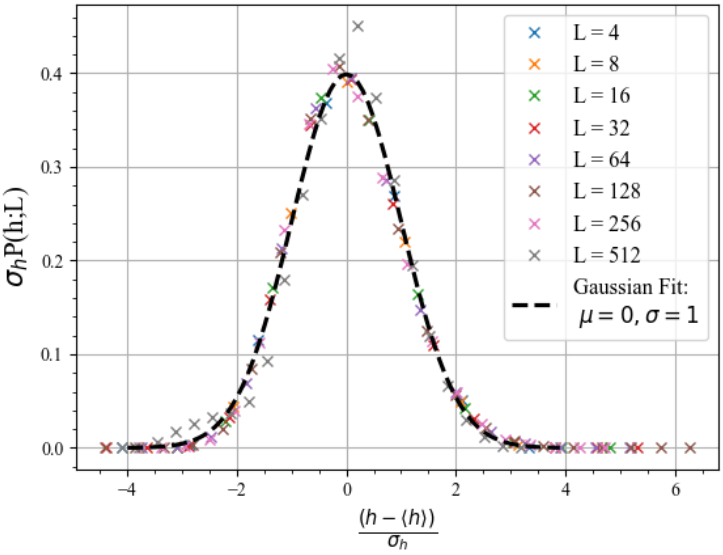

(b) Data collapse plot

Figure 10: Figure (a) showing how the height probability, P(h;L) evolves as a function of h for different system sizes.The figure shows that as h increases the maximum P(h;L) decreases and this would be due to large system sizes having a greater range of heights. Figure (b) shows the collapsed data points for the height probability, figure 11, that has been normalised and centred about 0 . The figure also shows a Gaussian distribution with a mean value, $\mu = 0$ and standard deviation, $\sigma = 1$. The figure implies that the data does not corroborate with the theoretical assumption that the data can be modelled as a Gaussian distribution as all systems show deviation from the normal distributions.

from the Gaussian . This implies that the initial assumption about z_i are incorrect as z_i is dependent on adjacent sites . The kurtosis and skewness test was used as a numerical test to corroborate the findings. The Kurtosis is a measure of how differently shaped are the tails of a distribution compared to a normal distribution, with a kurtosis of 0. The skewness focuses on the overall shape of the distribution compared to the normal distribution, with a skewness of 0.

Numerical Tests		
Data	Avg Kurtosis	Avg Skewness
Scaled Probability	-0.62	0.91
Scaled Heights	0.1	0.91

Table 2: Kurtosis and skewness test performed on the collapsed probability and scaled height for system sizes L = 4, 8, 16 , 32, 64, 128, 256, 512. The Kurtosis and skewness of a normal distribution is 0. The figure shows that the average kurtosis and skewness for both data types deviate from the normal distribution. The figure implies that both data types cannot be modelled as a Gaussian and corroborate the results from figure 10 (b).

Table 2 shows that the scaled probability and the scaled height deviate from the expected values of both the Kurtosis and skewness test. The results imply that the data cannot be modelled by a Gaussian hence corroborate the findings discussed above.

4 The avalanche-size probability

This section focus on the measuring of the avalanche-size probability, P(s;L) and associated moments for a system in the steady state.

4.1 Task 3a part (a)

Task 3a part (a) plots the avalanche-size probability defined as,

$$P_N(s;L) = \frac{No.\ of\ avalanches\ of\ size\ s\ in\ a\ system\ of\ size\ L}{Total\ no.\ of\ avalanches} \tag{16}$$

against the avalanche size s utilising the log-binned data. The data for the system sizes is run for reasonably large N. To process the data, the scale of the log-binned data is set to 1.5. This is to reduce the noise present in the tail of P where the statistics are generally poor, especially for sample sizes of N = 10^4.

4.1.1 Results

Figure 11 shows the cutoff avalanche size s_c, which is the component of each system that decays rapidly. s_c increases with the L and the probability of a larger avalanche increases with the L. P(s;L) can be approximated by a power-law decay of the form, P(s;L) $\propto s^{-\tau_s}$ for $1 << s << s_c$ where τ_s is the avalanche-size exponent.

4.2 Task 3a part (b)

Task 3a part (b) investigates the consistency of P(s; L) with the finite-size scaling ansatz,

$$\tilde{P_N}(s;L) \propto s^{-\tau_s}\mathcal{G}\left(\frac{s}{L^D}\right) \tag{17}$$

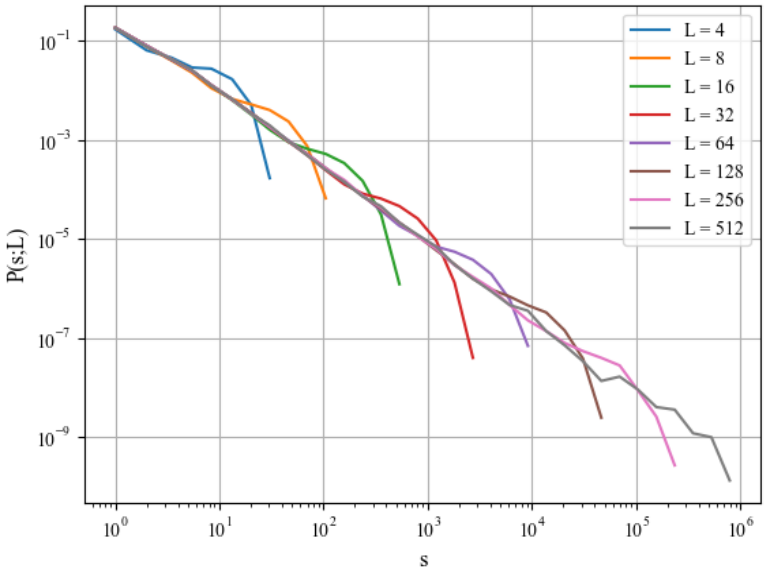

Figure 11: Avalanche size probability , P(s; L) as a function of the avalanche size s on a log log axis. The plot shows numerical data for L = 4, 8, 16, 32, 64, 128, 256 and 512. The figure implies that the cutoff avalanche size, s_c, increases with system size and the probability of larger avalanches increases for larger systems.

and to estimate the values of the avalanche dimension, D and τ_s through a data collapse. Figure 11 shows a bump on each systems curve followed by a rapid decay in P(s;L). These bumps can be collapsed by plotting $P(s;L)s^{\tau_s}$ as a function of $\frac{s}{L^D}$ The curves will collapse onto the graph for the scaling function $\mathcal{G}$. Plotting Log(s_c) (here the maximum avalanche) as a function of the Log(L) will produce a linear fit with the gradient = D. τ_s is estimated using a system size L = 512 by plotting the log(P) against the log(S) where the gradient of the line is -τ_s.

4.2.1 Results

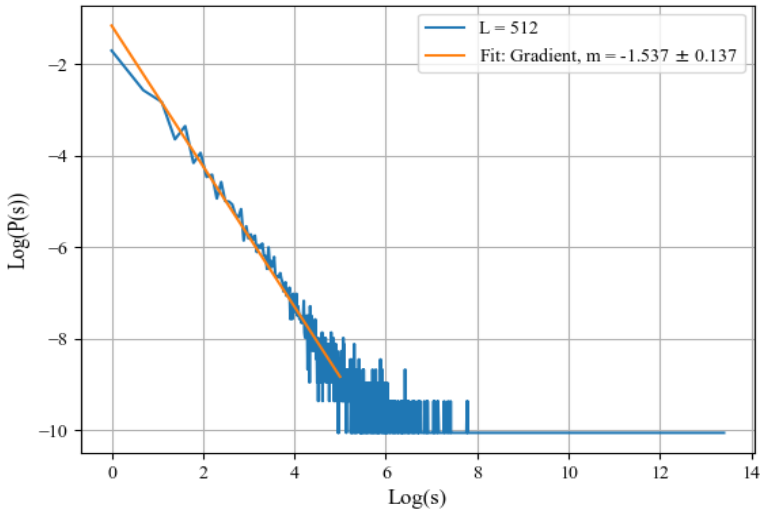

Figure 13: Avalanche probability, showing the Logarithm of P as a function of the logarithm of s for the system size L = 512. The plot shows a linear fit through the decaying component of the probability where the gradient, m = -1.537 ± 0.137. The avalanche size exponent is -m and hence the estimated value of the avalanche-size exponent, τ_s = 1.537 ± 0.137.

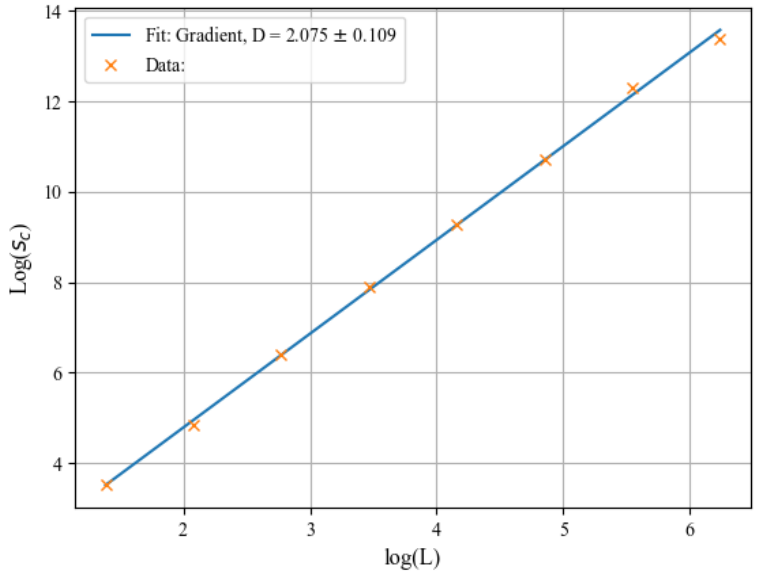

Figure 12: Avalanche-size cutoff, shows Logarithm of s_c as a function of logarithm of L. The figure shows a linear fit with gradient, D = 2.075 ± 0.109, this represents the value of the avalanche dimension.

The avalanche-size cutoff plot, figure 12, show that the D = 2.075 ± 0.109. Figure 13, shows that the avalanche-size exponent, $\tau_s = 1.537 \pm 0.137$.

The data collapse plot, figure 14 shows that all systems have been collapsed onto a single curve which represents the scaling function $\mathcal{G}$. This shows that $P_N(s; L)$ is consistent with the finite-size scaling ansatz discussed in equation (17).

4.3 Task 3b

Task 3b investigates the kth moment, which describes how the average avalanche size diverges as the system size tends to infinity. The task also uses moment scaling analysis to estimate the values of D and τ_s This task requires the direct measurement of the kth moment defined as,

$$\langle s^k \rangle = \lim_{T \to \infty} \frac{1}{T} \sum_{t=t_0+1}^{t_o+T} s_t^k \tag{18}$$

where s_t is avalanche size in the steady state .Using the finite-size scaling ansatz, equation (17), higher moments can be calculated. In the limit for L tending to infinity the scaling of the kth moment of the avalanche-size probability is,

$$\langle s^k \rangle \propto L^{D(1+k-\tau_s)} \tag{19}$$

for $k >> 1$ and $L >> 1$. The moment analysis method determines D and τ_s by analysing the scaling of the moments of the P(s; L). Taking the logarithm of equation (19) we get,

$$Log\langle s^k \rangle = D(1 + k - \tau_s)Log(L) + C \tag{20}$$

where c is a constant. Plotting Log($\langle s^k \rangle$) as a function of Log(L) for k = 1, 2, 3, 4, the gradient for each k will be equivalent to D(1 + k - τ_s) . D(1 + k - τ_s) is then plotted as a function of k and the resulting linear fit will have a gradient = D and τ_s = 1 + k, where k is the x-axis intercept. The critical exponents, D and τ_s must satisfy the scaling relation for the boundary driven condition,

$$D(2 - \tau_s) = 1 \tag{21}$$

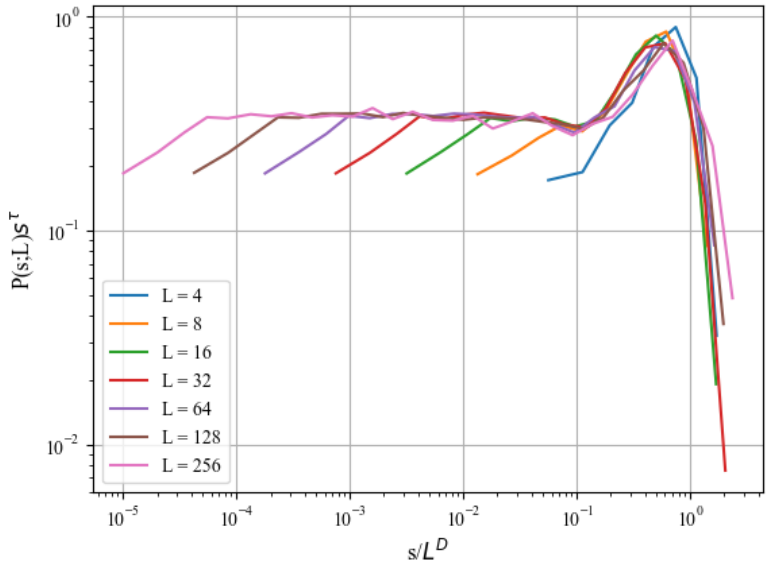

Figure 14: Data collapse , showing P(s;L)s_s^{τ} as a function of $\frac{s}{L^D}$. The figure shows the collapsed curves for the system sizes L = 4, 8, 16, 32, 64, 128, 256 and 512. The shows that all systems have been collapsed onto a single curve. This curve represents the scaling function $\mathcal{G}$.

4.3.1 Results

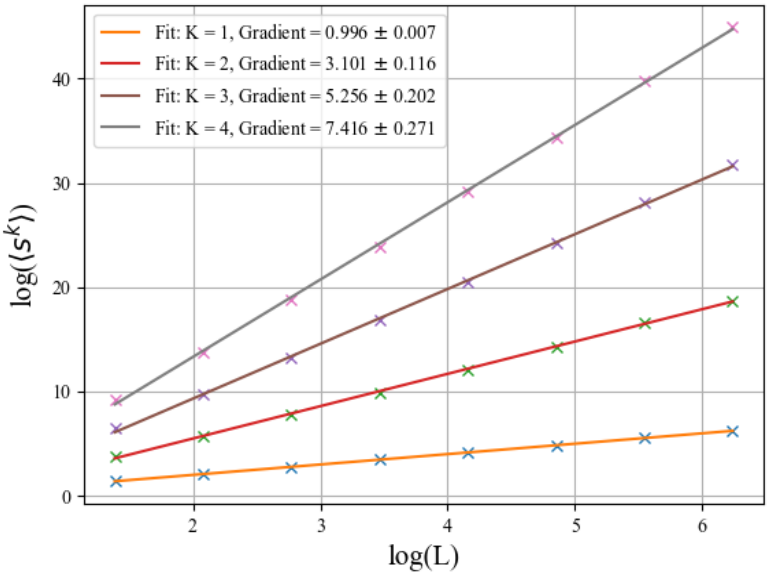

Figure 15: Average avalanche plot showing how the logarithm of the kth moment, Log($\langle s^k \rangle$) as a function of Log(L) for k = 1, 2, 3, 4. The figure shows four linear fits, each representing a k value. The figure shows the gradients for each k that is used to calculate the values for D and τ_s.

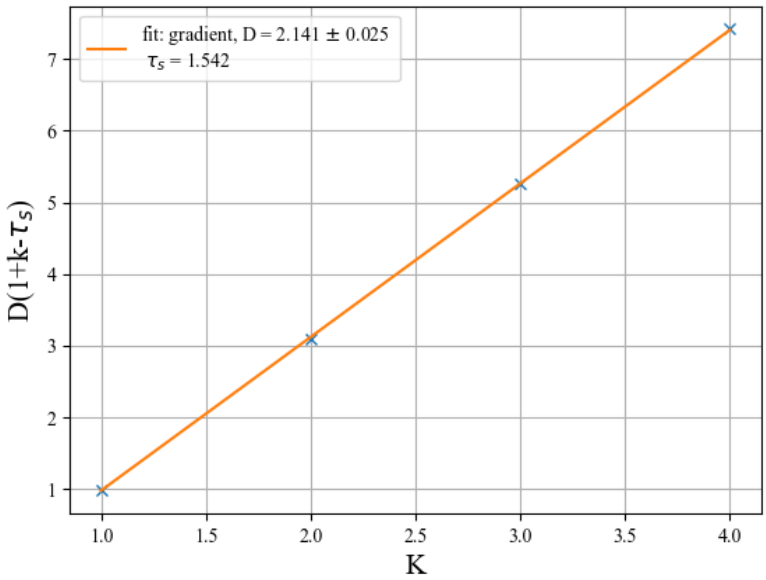

Figure 16: Kth Moment plot showing the estimated exponent, D(1+k - τ_s) as a function of k. The gradient of the fit, D = 2.141 ± 0.025 and the avalanche exponent, τ_s = 1.542 calculated from the x-axis intercept.

Figure 15 shows Log($\langle s^k \rangle$) as a function of Log(L) for k = 1, 2, 3, 4. Figure 16 shows D(1 + k - τ_s) as a function of k. The figure shows a linear fit with a gradient, D =2.141 ± 0.025 and the avalanche exponent, τ_s = 1.542, obtained from the x-axis intercept. These results corroborate with the values estimated from Task 3a derived from the finite-size scaling ansatz data collapse. The scaling relation shown in equation (21) is = 0.98 ± 0.025. The result remains consistent with the expected behaviour of a boundary driven system.

5 Conclusion

The aim of the report was to study the behaviour of the Oslo model algorithm and to understand the avalanche probability, general framework of data collapse and the consistency of the results with systems displaying self-organised criticality. The results discussed in the report show that the Oslo model and the system self-organises into a steady state and demonstrates scale-free behaviour when taking the system size to infinity demonstrated by the avalanche-size probability. The results produced in the report show that the avalanche-size probability can be approximated as a power-law decay and corroborates with the theoretical framework that describes self-organised criticality and remains consistent with results.

References

[1] T.S. Evans, *Slides for Networks course*, Physics Dept., Imperial College London, 2014, downloaded from Blackboard 2nd February 2015.

[2] K.Christensen and N.Maloney, *Complexity and Criticality*, Imperial College Press, London, 2005.

[3] T.S. Evans and R. Lambiotte, "Line Graphs, Link Partitions and Overlapping Communities", Phys.Rev.E. **80** (2009) 016105.